Nonequilibrium relaxation analysis of two-dimensional melting

Hiroshi Watanabe,[1] Satoshi Yukawa,[1] Yukiyasu Ozeki,[2] and Nobuyasu Ito[1]
[1]*Department of Applied Physics, School of Engineering, The University of Tokyo, Hongo, Bunkyo-ku, Tokyo 113-8656, Japan*
[2]*Department of Physics, Meguro-ku, Tokyo Institute of Technology, Oh-okayama, Tokyo 152-8551, Japan*
(Received 24 June 2002; published 24 October 2002)

The phase diagram of a hard-disk system is studied by observing nonequilibrium relaxation functions of a bond-orientational order parameter using particle dynamics simulations. From a finite-time scaling analysis, two Kosterlitz-Thouless transitions can be observed when the density is increased from the isotropic fluid phase to closest packing. The transition densities are estimated to be 0.901(2) and 0.910(2), where the density denotes the fraction of area occupied by the particles, the density is normalized to one for the quadratic packing configuration. These observations are consistent with the predictions of the Kosterlitz-Thouless-Halperin-Nelson-Young theory.

DOI: 10.1103/PhysRevE.66.041110 PACS number(s): 64.60.−i, 64.70.Dv, 02.70.Ns

I. INTRODUCTION

Since computer simulation suggested a melting transition in hard-particle system [1,2], many studies have been undertaken to understand the nature of this transition, which is now often called as the ''Alder transition.'' The property of the two-dimensional solid of the hard-disk system is not clear yet, as the two-dimensional system with short-range interaction at density less than 1 lacks positional order [3]. Halperin and Nelson [4], and Young [5] explained the two-dimensional solid based on the Kosterlitz-Thouless (KT) transition, which is referred to the Kosterlitz-Thouless-Halperin-Nelson-Young (KTHNY) theory. The KTHNY theory introduced a new phase, a ''hexatic phase,'' between the liquid and the solid phase. The correlation of the bond-orientational order is long-range in the solid phase, quasi-long-range in the hexatic phase, and short-range in the liquid phase [6]. With the assumption that two kinds of topological defects, a disclination and a dislocation, are unbound separately, the theory predicts two KT transitions. Another theory was proposed by Chui [7]. He studied the spontaneous generation of grain boundaries, and predicted a first-order transition.

To clarify the nature of this transition, many computer simulations have been performed. Alder and Wainwright reported that the transition is of first order in their particle dynamics simulations with 870 particles. The densities were normalized to 1 for the quadratic packing configuration, so $\rho=4Nr^2/A$ with the area of the system A, the number of particles N, and the radius of the particles r. Hereafter we use the definition for density. They determined the highest density at which the isotropic phase can exist as $\rho_i=0.880$ and the lowest one at which the solid phase can exist as $\rho_m=0.912$ [2]. Zollweg, Chester, and Leung examined the size dependence in the hard-disk systems and found a logarithmic size dependence close to one of the melting points [8]. They also argued that when the system becomes larger, the density range of the intermediate phase becomes smaller, so it is not clear whether the intermediate phase, which corresponds to the hexatic phase in the KTHNY theory, survives or vanishes in the thermodynamic limit. Lee and Strandburg found double peaks in a distribution range of volumes obtained by Monte Carlo (MC) simulations with constant pressure [9]. With Lee-Kosterlitz scaling, they found a bulk free-energy barrier between two phases and concluded that the transition is of first order. As they used only up to 400 particles, it is difficult to say whether the system is large enough to extrapolate to the thermodynamic limit. Fernandez, Alonso, and Stankiewicz reported that the two transition points ρ_i and ρ_m were the same within statistical errors [10]. They obtained $\rho_i=\rho_m=0.916(5)$ for the transition density and concluded that the intermediate phase does not exist or its range is quite small. Weber, Marx, and Binder studied the transition via the sub-block analysis method of finite-size scaling and concluded that the transition is of first order [11]. They obtained the critical densities $\rho_i=0.880$ and $\rho_m=0.905$. Jaster studied the divergence of the bond-orientational correlation length and the susceptibility with MC simulations and obtained the results that are in good agreement with the KTHNY theory [12]. He determined the critical densities as $\rho_i=0.899(1)$ and $\rho_m\geqslant 0.91$. Recently, Sengupta, Nielaba, and Binder studied a dislocation-free triangular solid of hard disks by MC simulations [13].

They found that the KTHNY transition preempts the first-order transition by a small margin with numerical solutions of KTHNY recursion relations. Though many papers have been dedicated to the problem, as yet there are no conclusive results to explain the transition.

In this paper, we study the problem by analyzing the nonequilibrium relaxation (NER) behavior of the bond-orientational order using particle dynamics simulations. By analyzing the NER data, one can accurately determine transition points and exponents including dynamical exponents for various kinds of systems with the MC method [14–16]. NER was also applied to spin-glass transitions to analyze the equilibrium phase diagram [17]. These studies showed that equilibrium properties of a system can be studied by analyzing its NER behavior. NER methods saves much computational time because they use only the relaxation interval which cannot be used by equilibrium methods but which occurs, nevertheless, in the simulations. Therefore the equilibrium state of the system does not have to be reached. In addition, it turns out that the NER methods less influenced by finite-size effects.

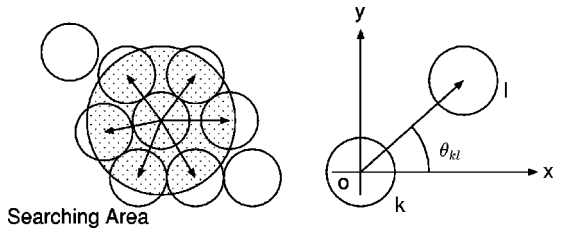

FIG. 1. The definition of the neighboring angle θ_{kl} and the number of neighboring particles n_k, where k is a particle index and l is an index of the neighboring particles. The value of θ_{kl} is defined as the angle between the line from particle k and l with respect to an arbitrary, but fixed global axis. The value of n_k is the number of particles in the search area of the particle k.

II. BOND-ORIENTATIONAL ORDER

The bond-orientational order ϕ_6 is defined as

$$\phi_6 = \left| \frac{1}{N} \sum_k^N \sum_l^{n_k} \frac{e^{6i\theta_{kl}}}{n_k} \right|^2, \tag{1}$$

where N and n_k denote the number of particles and the number of neighbors of particle k, respectively. The definition of n_k and θ_{kl} are described in Fig. 1. Note that the angle θ_{kl} is defined with respect to an arbitrary but fixed global axis. To search neighboring particles, we use a search area within a circle with radius R and ignore particles at long distance to save computer time, in contrast to Jaster, who uses the Voronoi construction [12]. The value of R is set to $2.7r$ (r is the radius of particles), to find not more than six neighbors in the area. We confirmed that the value of ϕ_6 has about the same value for the Voronoi construction and our searching area method. The parameter ϕ_6 becomes 1 when particles are located on the points of a hexagonal grid, and it becomes 0 when the particle location is completely disordered. Therefore ϕ_6 can be used to describe how close the system is to hexagonal packing. The expectation value of ϕ_6 depends on density ρ and in nonequilibrium on time t.

III. NUMERICAL SIMULATION

A. The model

We monitor the time evolution of ϕ_6 at various densities in particle dynamics simulation with periodic boundary conditions. The fifth-order predictor-corrector method are used for the time integration. We treat elastic disks and extrapolate to the hard disks. All properties are rescaled with a radius, mass and mean kinetic energy of particles, so all quantities are dimensionless. The number of particles N of the system was 23 256. The density of the system is controlled by choosing the value of the radius of particles r. The mass of the particles m was set to 1, and the mean kinetic energy per particle $\langle v^2/N \rangle$ was set to 12.8. Under this condition, the Young's modulus was set to 10^6 to ensure that the penetration depth is smaller than $0.02r$. The extrapolation to hard-core systems can be done by calculating an effective radius

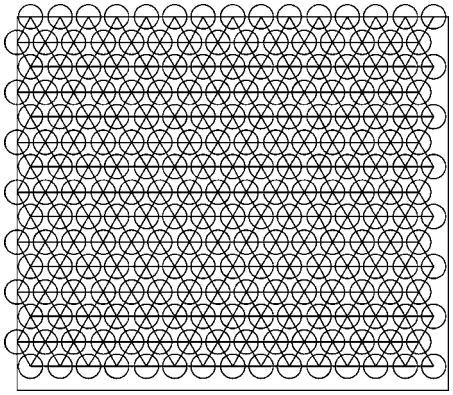

FIG. 2. The initial configuration of a system with 225 particles, and density $\rho = 0.89$. All quantities are dimensionless. A small system is shown to improve visibility. Circles represent particles, and the lines are bonds to calculate the hexatic packing order parameter ϕ_6 having a value of 1.

r' that is smaller than the real radius r used for the simulation [18]. The effective density ρ is extrapolated for the hard-core system as

$$\rho = \frac{4Nr'^2}{A}, \tag{2}$$

where A is the area in which the particles are allowed to move and N is the number of particles in the system. In the following, we use this effective density. A time step was set to be 1.0×10^{-4}, which is short in comparison to the theoretical mean contacting time, which is about 10^{-3} in this case, to make the numerical integration stable. The theoretical mean contacting time is the time when two particles are in contact, and it can be calculated by the elastic modulus and the mean velocity of particles. Total simulational steps are 900 000. The studied range of density from 0.87 to 0.94 was the range the Alder transitions occur; 10–64 runs are averaged for each density.

At the beginning of the simulation, the particles were set up in the perfect hexagonal order, in other words, $\phi_6(t=0,\rho)$ is 1, and the particles are given an initial velocity in random direction. This initial configuration is shown in Fig. 2. In this condition, the asymptotic behavior of $\phi_6(t,\rho)$ is expected to be an exponential decay in the disordered (fluid) phase, a power-law decay in the KT (hexatic) phase and a decay slower than power law in the ordered (solid) phase.

B. Results

A typical configuration of small system, $N=225$, is shown in Fig. 3 and the time evolution of ϕ_6 with $N=23\,256$ is shown in Fig. 4. Figure 4 shows that ϕ_6 becomes asymptotically constant at high density in the solid phase and decays exponentially at low density in the liquid phase. The KTHNY theory predicts the range of density in which ϕ_6 shows power-law decay between the solid and the liquid phase, but this is not clear from Fig. 3.

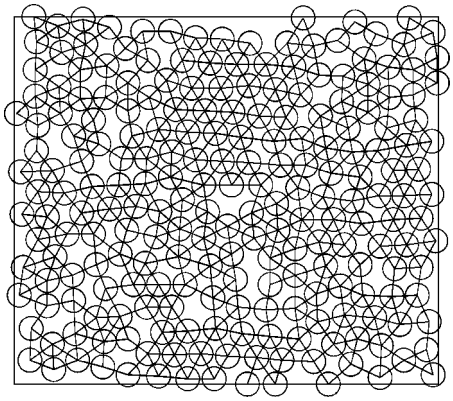

FIG. 3. Typical configuration of a system with 225 particles, a scaled density $\rho=0.89$, and a hexagonal packing order parameter $\phi_6=0.182$. A small system is shown in order to improve visibility.

C. Finite-time scaling analysis

Although it is not easy to estimate the transition densities ρ_i and ρ_m from Fig. 4, we can evaluate them from finite-time scaling. The following finite-time scaling analysis is useful to study the KT transition [19,20]. For densities lower than ρ_i, a characteristic relaxation time τ exists in the system, so we can write $\phi_6(\rho,t)$ as

$$\phi_6(\varepsilon,t)=t^{-\lambda}\overline{\phi_6}(t/\tau)\left(\varepsilon=\frac{\rho-\rho_i}{\rho_i}\right), \tag{3}$$

with a critical exponent λ.

We cannot scale the data of densities higher than $\rho>\rho_i$ because there is no characteristic relaxation time as in the system with critical KT behavior.

According to the prediction of the KTHNY theory, the correlation length ξ diverges exponentially at the KT transition point, so it has the form as $\xi\sim\exp(d/\sqrt{\varepsilon})$, with a constant d. Assuming the scaling relation $\tau\sim\xi^z$ with a dynamical exponent z [19,20], the divergence behavior of τ can be written as

$$\tau(\varepsilon)=b\,\exp(a/\sqrt{\varepsilon}), \tag{4}$$

with constants a and b. Using Eqs. (3) and (4), we obtain the finite-time scaling function $\overline{\phi_6}$ as

$$\phi_6(\varepsilon,t)=t^{-\lambda}\overline{\phi_6}(te^{-a/\sqrt{\varepsilon}}). \tag{5}$$

One can apply the same argument to determine ρ_m. We analyze the results of ϕ_6 with the scaling form Eq. (5). Scaling parameters are the critical densities ρ_i and ρ_m, the critical exponent λ, and the proportionality constant a of Eq. (4).

The scaling plot of the liquid hexatic transition is shown in Fig. 5. Parameters are $\rho_i=0.901(2)$, $\lambda=0.2(1)$, and $a=0.83(1)$. We take $t\exp(-a/\sqrt{\varepsilon})$ as the horizontal axis and $\phi_6(\varepsilon,t)t^{\lambda}$ as the vertical. The graphs for the densities lower than 0.901 are well scaled, but those of higher densities are not. This feature is characteristic to the KT transition [19,20].

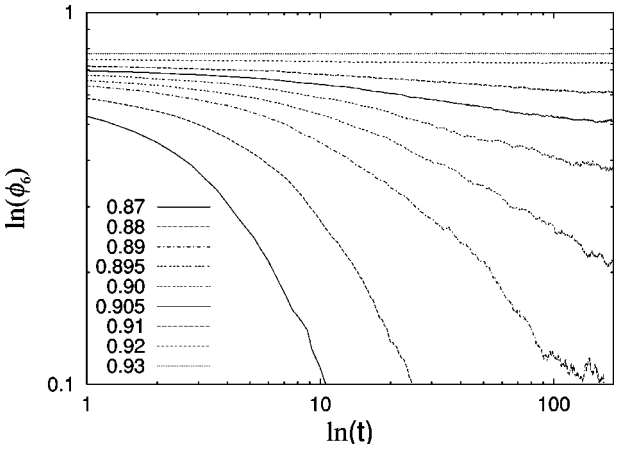

FIG. 4. The time evolutions of the hexatic-ordering parameter ϕ_6 (log-log plot). The asymptotic behavior of ϕ_6 becomes constant at high density and decays exponentially at low density. The graphs correspond to the solid and the liquid phases, respectively. As predicted by the KTHNY theory, the density range in which ϕ_6 shows power-law decay is between the solid and the liquid phases, but it cannot be determined from this figure.

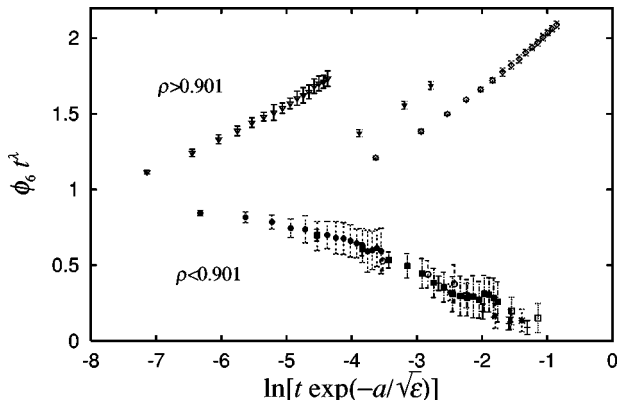

FIG. 5. Finite-time scaling with $\rho_i=0.901$, $\lambda=0.2$, and $a=0.83$. The data of lower densities ($\rho<\rho_i$) fall on a single curve, but the data of higher densities do not show the scaling behavior. Densities are 0.878, 0.881, 0.883, 0.885, 0.888, 0.890, 0.893, 0.898, 0.903, 0.907, 0.913, and 0.918.

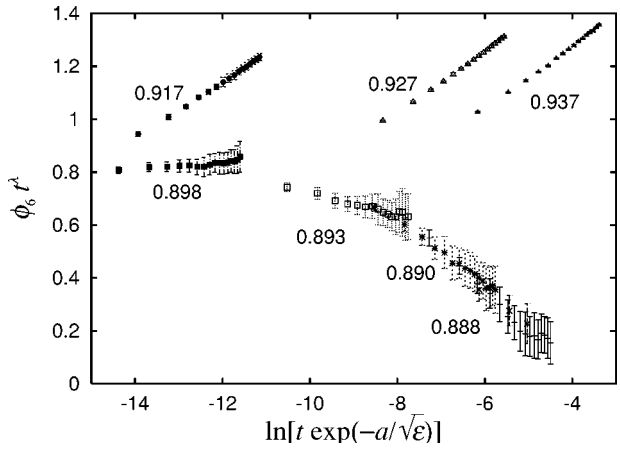

FIG. 6. Finite-time scaling with $\rho_m=0.910$, $\lambda=0.1$, and $a=1.2$. The data of lower densities ($\rho<\rho_m$) fall on a single curve, but data of higher densities do not.

The fit result for the hexatic-solid transition is shown in Fig. 6. Parameters are $\rho_m = 0.910(2)$, $\lambda = 0.1(1)$, and $a = 1.2(1)$. The data at lower densities show good scaling behavior while the data of higher densities do not, which also suggests a KT transition.

One can determine these two critical densities uniquely, since they cannot be scaled by any λ and a with different critical densities used above. Jaster estimated these two transition points as $\rho_i = 0.899(1)$ and $\rho_m \geqslant 0.91$ [12]. Our results are consistent with his result.

IV. SUMMARY

We have studied the nonequilibrium relaxation behavior of the bond-orientational order in the two-dimensional hard-core system with the particle dynamics simulations, and we supported the existence of the hexatic phase. Using finite-time scaling analysis, two KT-transition points are determined as $\rho_i = 0.901(2)$ and $\rho_m = 0.910(2)$. The scaling behavior only at lower density of the two transition points suggests that these transitions are of the KT-transition type. These results show good agreement with the KTHNY theory. This study also shows that the NER method can be used for the particle dynamics simulation as well as for the Monte Carlo method.

ACKNOWLEDGMENTS

We thank S. Miyashita for fruitful discussions and H.-G. Matuttis for great help with debugging the code. The simulations were performed using the facilities of the Supercomputer Center, Institute for Solid State Physics, University of Tokyo. This work was partially supported by the Japan Society of Science Grant Nos. 13740235 and 14540354.

[1] W. W. Wood and J. D. Jacobson, J. Chem. Phys. **27**, 1207 (1957).
[2] B. J. Alder and T. E. Wainwright, Phys. Rev. **127**, 359 (1962).
[3] N. D. Mermin and H. Wagner, Phys. Rev. Lett. **17**, 1133 (1966).
[4] B. I. Halperin and David R. Nelson, Phys. Rev. Lett. **41**, 121 (1978).
[5] A. P. Young, Phys. Rev. B **19**, 1855 (1979).
[6] K. J. Strandburg, Rev. Mod. Phys. **60**, 161 (1988).
[7] S. T. Chui, Phys. Rev. Lett. **48**, 933 (1982).
[8] J. A. Zollweg, G. V. Chester, and P. W. Leung, Phys. Rev. B **39**, 9518 (1989).
[9] J. Lee and K. J. Strandburg, Phys. Rev. B **46**, 11 190 (1992).
[10] J. F. Fernandez, J. J. Alonso, and J. Stankiewicz, Phys. Rev. Lett. **75**, 3477 (1995).
[11] H. Weber, D. Marx, and K. Binder, Phys. Rev. B **51**, 14 636 (1995).
[12] A. Jaster, Phys. Rev. E **59**, 2594 (1999).
[13] S. Sengupta, P. Nielaba, and K. Binder, Phys. Rev. E **61**, 6294 (2000).
[14] N. Ito, Physica A **196**, 59 (1993).
[15] N. Ito, Physica A **192**, 604 (1993).
[16] N. Ito, K. Fukushima, K. Ogawa, and Y. Ozeki, J. Phys. Soc. Jpn. **69**, 1931 (2000).
[17] Y. Ozeki and N. Ito, Phys. Rev. B **64**, 024416 (2001).
[18] W. Vermöhlen and N. Ito, Phys. Rev. E **51**, 4325 (1996).
[19] Y. Ozeki, K. Ogawa, and N. Ito (unpublished).
[20] Y. Ozeki and N. Ito, in *Proceedings of the Computer Simulation Studies in Condensed Matter Physics XV*, edited by D. P. Landau, S. P. Lewis, and H.-B. Schüttler (Springer-Verlag, Berlin, 2002).